Uncoupling protein 2 is upregulated in melanoma cells and contributes to the activation of Akt/mTOR and ERK signaling

JINRAN LI[1,2], YUXI JIA[1], LIN AN[1], CHUNBO NIU[3], XIANLING CONG[1] and YUNFENG ZHAO[2]

[1]Department of Dermatology, China-Japan Union Hospital, Jilin University, Changchun, Jilin 130033, P.R. China; [2]Department of Pharmacology, Toxicology and Neurosciences, LSU Health Sciences Center, Shreveport, LA 71130, USA; [3]Department of Pathology, China-Japan Union Hospital, Jilin University, Changchun, Jilin 130033, P.R. China

Received July 5, 2019; Accepted December 12, 2019

DOI: 10.3892/ijo.2020.5010

Abstract. The aim of the present study was to characterize the expression of uncoupling protein 2 (UCP2) in melanoma and to study the potential mechanisms underlying the involvement of UCP2 in melanomagenesis using human melanoma cell lines. The expression of UCP2 was evaluated in specimens from normal control subjects, patients with compound nevus, and patients with cutaneous and mucosal melanoma. Stable knockdown of UCP2 was achieved in human melanoma cell lines, which were used to examine whether UCP2 knockdown affects the mitochondrial membrane potential and intracellular levels of ATP, reactive oxygen species and lactate. Cell proliferation, invasion, spheroid formation and cisplatin sensitivity were also evaluated in the UCP2 knockdown cells. Finally, the effects of UCP2 knockdown on the Akt/mammalian target of rapamycin (mTOR) and extracellular signal-regulated kinase (ERK) pathways, which are important oncogenic pathways during melanomagenesis, were evaluated. Relatively high expression of UCP2 was detected in human melanoma specimens, which was correlated with Clark level and Breslow thickness. Knockdown of UCP2 suppressed cell proliferation, invasion and spheroid formation, and increased the sensitivity of melanoma cells to cisplatin. Furthermore, the UCP2 knockdown cells exhibited inhibition of Akt/mTOR signaling and ERK activation. Therefore, human melanoma tissues exhibit relatively high UCP2 expression, which may be implicated in the mechanisms underlying tumor progression. The potential role of UCP2 in melanomagenesis may involve enhancing the Akt/mTOR and mitogen-activated protein kinase/ERK pathways.

Correspondence to: Dr Yunfeng Zhao, Department of Pharmacology, Toxicology and Neurosciences, LSU Health Sciences Center, 1501 Kings Highway, Shreveport, LA 71130, USA
E-mail: yzhao1@lsuhsc.edu

Dr Xianling Cong, Department of Dermatology, China-Japan Union Hospital, Jilin University, 126 Xiantai Street, Changchun, Jilin 130033, P.R. China
E-mail: congxl@jlu.edu.cn

Key words: uncoupling protein 2, melanoma, Akt, extracellular signal-regulated kinase, invasion, metabolism

Introduction

Melanoma originates from melanocytes and is the most aggressive type of skin cancer, accounting for the majority of skin cancer-related deaths, despite only accounting for 1-2% of all skin cancers (1). Melanomagenesis has been attributed to melanocytic nevi (2), genetic factors (3) and ultraviolet light exposure (4), although the underlying molecular mechanisms have yet to be fully elucidated.

Uncoupling proteins (UCPs) are anion carriers located in the mitochondrial inner membrane, where they facilitate anions crossing the inner membrane, thereby allowing protons back to the matrix and reducing the mitochondrial membrane potential (5). In humans, the UCP family includes five members: UCP1 is mainly expressed in brown adipose tissue (6), UCP2 is ubiquitously expressed (7), UCP3 is mainly expressed in the heart and skeletal muscle (8), and UCP4 and UCP5 are only expressed in the brain (9,10). The UCP2 protein has been studied in human diseases and was found to be involved in diabetes, cardioprotection, neuroprotection, carcinogenesis, and the immune response (5). The tumor-promoting effect of UCP2 is attributed to its regulation of the cellular redox status, which allows it to promote cancer cell growth (7) and a metabolic shift from oxidative phosphorylation to glycolysis and glutaminolysis (7,11). For example, an altered cellular redox status can affect redox-sensitive kinase signaling, with UCP2 deficiency in progenitor cells decreasing cell proliferation via inactivation of mitogen-activated protein kinase (MAPK)/extracellular signal-regulated kinase (ERK) signaling (12). Furthermore, inhibition of UCP2 in human pancreatic cancer cells causes an increase in reactive oxygen species (ROS), which activates the protein kinase B (Akt)/mammalian target of rapamycin (mTOR) pathway (13).

In our previous study using UCP2 knockout mice, UCP2 was found to promote chemically induced skin carcinogenesis *in vivo* (14). In the JB6 P+ skin cell transformation model, overexpression of UCP2 promoted glycolytic flux by activating the Akt pathway (15) and enhanced skin cell transformation by activating PLC-γ1 signaling (16). However, it remains unclear whether UCP2 plays a role in melanoma, which is the deadliest type of skin cancer. Therefore, the aim of the present study was to evaluate whether inhibition of UCP2 could be useful for treating melanoma and, to the best of our knowledge, it is

the first study to compare UCP2 expression in specimens from normal skin, compound nevus and melanoma. The hypothesis was that UCP2 would be relatively highly expressed in melanoma tissues and that its levels would be negatively associated with the patient's prognosis. In addition, human melanoma cells with stable knockdown of UCP2 were generated in order to investigate its potential mechanism(s) of action.

Materials and methods

Patients and tissue samples. The protocol of this retrospective study was approved by the Institutional Review Board of China-Japan Union Hospital, Jilin University. Specimens were collected from 81 consecutive patients who were diagnosed with skin and mucosal melanoma at the Department of Pathology (China-Japan Union Hospital) between September 2016 and December 2018. Informed consent was obtained from patients at the time of sample collection. The diagnosis had been established based on pathological examination following complete surgical excision of the lesion. The eligibility criteria included i) age 18-80 years and ii) primary skin lesion without a history of radiotherapy or chemotherapy. The exclusion criteria included overweight status (body mass index >25 kg/m^2), diabetes, and concomitant tumors, as elevated UCP2 expression may be associated with these conditions. Based on these criteria, the present study included 65 patients (33 men and 32 women) with cutaneous (n=52) and mucosal (n=13) melanoma. For comparison, control skin tissues were obtained from 49 healthy individuals who had undergone cosmetic surgery (control group) and surgical specimens were also collected from 51 healthy individuals who had undergone excision of compound nevus (compound nevus group). The clinical characteristics of the patients are summarized in Tables I and II.

Cell culture and reagents. Human melanoma A375 cells were purchased from the American Type Culture Collection (CRL-1619). Human melanoma SK-Mel-28 cells were kindly provided by Dr Stephan Witt from our institution (originally purchased from the American Type Culture Collection). A375 cells are more aggressive compared with SK-Mel-28 cells (17). The cells were grown in RPMI-1640 medium supplemented with 10% fetal bovine serum (Atlanta Biologicals, Inc.) and 1 mM sodium pyruvate, which was maintained at 37˚C in a humidified incubator (95% air and 5% CO_2). Mycoplasma testing was routinely performed for the cell lines.

UCP2 shRNA lentivirus (LVPi026640) and scramble shRNA lentivirus (LVP015G) were purchased from Applied Biological Materials. Both vectors contained a green fluorescent protein (GFP) tag. The target sequences were as follows: 5'-CGGTTACAGATCCAAGGAGAA-3', 5'-GGCCTGTATGATTCTGTCA-3', 5'-GCACCGTCAATGCCTACAA-3' and 5'-CGTGGTCAAGACGAGATACATGAACTCTG-3'. JC-1 dye was purchased from Cayman Chemicals (cat. no. 15003).

Antibodies and reagents. All primary antibodies were diluted at a ratio of 1:1,000. Antibodies to β-actin (cat. no. sc-47778), ERK (cat. no. sc-94), and phosphorylated ERK (p-ERK; cat. no. sc-7383) were purchased from Santa Cruz Biotechnology, Inc. Antibodies to p-4E-BP1 (cat. no. 13396), 4E-BP1 (cat. no. 9452), p-Akt (cat. no. 9275), Akt (cat. no. 2920), p-p70S6K (cat. no. 9205) and p70S6K (cat. no. 9202) were purchased from Cell Signaling Technologies, Inc.

Establishing the UCP2 KD melanoma cells. A375 and SK-Mel-28 cells were seeded in 24-well plates (20,000 cells/well). On the next day, a cell infection mixture was prepared: 10 MOI viruses per 1 ml of culture medium plus 2 μl of polybrene (4 μg/μl). The cell culture medium was then removed and replaced with 500 μl of the cell infection mixture. After 24 h, the infection mixture was replaced with fresh culture medium and the cells were incubated at 37˚C for another 24 h before the addition of medium with puromycin (1 μg/ml). Clonal selection lasted for 12 days with the puromycin-containing medium replaced once every 3 days. The scramble shRNA-infected clones were enriched via sorting of GFP-positive cells using flow cytometry and collected in bulk, whereas the UCP2 knockdown (KD) clones were collected as single cells via GFP sorting using flow cytometry. The UCP2 KD clones were expanded and western blot analysis was performed for selection.

MTT assay. The melanoma cells were seeded in 96-well plates (6,000 cells/well) and cultured at 37˚C overnight. The cells were then treated using various cisplatin concentrations (15, 5, 1.67, 0.56, 0.19 and 0 μM). Cisplatin has been approved for the treatment of metastatic melanoma in the U.S. (18). Cisplatin (cat. no. 1134357, Sigma-Aldrich; Merck KGaA) was dissolved in phosphate-buffered saline (PBS). After incubation at 37˚C for 48 h, cell viability was determined using the MTT assay (M5655; Sigma-Aldrich; Merck KGaA), with 10% MTT diluted in serum-free medium added to each well before a 4-h incubation at 37˚C. The MTT solutions were then replaced with dimethyl sulfoxide and the plates were shaken for 15 min at room temperature. The absorbance at 595 nm was then measured using a 96-well plater reader (Bio-Rad Laboratories, Inc.). All experiments were repeated at least three times.

Detection of mitochondrial membrane potential based on JC-1 staining. A total of 10,000 melanoma cells were seeded in 96-well plates. On the next day, the culture medium was replaced with fresh medium containing the JC-1 dye (2 μg/ml) and incubated at 37˚C for 30 min. The medium was then removed and the cells were washed once using PBS. The fluorescence intensities were measured immediately using a fluorescence spectrophotometer (JC-1 green: Ex=485 nm, Em=525 nm; JC-1 red: Ex=535 nm, Em=590 nm), and the ratio of JC-1 red vs. JC-1 green was used to evaluate the mitochondrial membrane potential. All experiments were repeated at least three times.

Detection of hydrogen peroxide levels. The Amplex Red Hydrogen Peroxide/Peroxidase Assay Kit (A22188, Molecular Probes; Thermo Fisher Scientific, Inc.) was used to measure intracellular hydrogen peroxide (H_2O_2) levels based on the manufacturer's instructions. The melanoma cells were grown in p100 dishes and collected via centrifugation (600 x g for 5 min) at room temperature. The cell pellets were then

Table I. Immunohistochemical expression of UCP2 in normal skin tissue, compound nevus tissue and skin mucosal melanoma tissues.

Tissue	n	UCP2 expression (n)		Positivity rate (%)
		Positive (n)	Negative (n)	
Normal control	49	1	48	2.0
Compound nevus	51	3	48	5.9
Melanoma	65	50	15	76.9

Red particle deposition in the cytoplasm was considered a positive finding. All other cases were considered negative. UCP2, uncoupling protein 2.

Table II. Association between UCP2 expression and the clinicopathological characteristics of skin melanoma.

Characteristics	n	UCP2 expression (n)			χ^2	P-value
		Negative	Mild	Strong		
Clark level					16.50	<0.001
I	1	1	0	0		
II	8	5		3	0	
III	7	2	5	0		
IV	18	3	10	5		
V	18	1	8	9		
Lymphocyte infiltration					3.5687	NS
No	14	2	8	4		
Yes	29	6	14	9		
Active	9	4	4	1		
Breslow thickness, cm					7.5038	0.0235
<0.5	25	9	11	5		
0.5-1.0	26	2	15	9		
>1.0	1	1	0	0		
Ulceration					3.6254	NS
Yes	33	9	18	6		
No	19	3	8	8		

P-values were determined using the χ^2 test. NS, not statistically significant (P≥0.05). UCP2, uncoupling protein 2.

suspended in 400 μl PBS containing proteinase inhibitors (cat. no. sc-29130, Santa Cruz Biotechnology, Inc.). The cells were then sonicated and the lysates collected via centrifugation at 4˚C (12,800 x g for 30 min). Freshly prepared cell lysates were filtered through 10K cut-off columns (82031-348, VWR) and the product's absorbance was measured at 560 nm using a 96-well plate reader. Background fluorescence was corrected by subtracting the value derived from the no-H_2O_2 control. All experiments were repeated at least three times.

Detection of lactate and ATP levels. Freshly prepared cell lysates were prepared as for the H_2O_2 assay and filtered through 10K cut-off columns before being used for both assays. The Lactate Colorimetric/Fluorometric Assay Kit (cat. no. K607-100, BioVision) was used to evaluate intracellular lactate levels, based on the absorbance at 570 nm measured using a 96-well plate reader. The ATP Luminescence Detection Assay Kit (cat. no. 700410, Cayman Chemicals) was used to evaluate intracellular ATP levels, based on the luminescence measured using a BioTek Multi-Mode microplate reader. All experiments were repeated at least three times.

Cell invasion assay. Invasion ability was evaluated using Transwell inserts (cat. no. 3422, Corning, Inc.) that were coated with 50 μg/ml of Matrigel. A total of 50,000 melanoma cells were suspended in serum-free medium and 100 μl of the cell suspension was transferred into the inserts, whereas complete growth medium was added to the bottom wells. The cells were then cultured for 12 h at 37˚C before the inserts were removed, fixed in 10% neutral-buffered formalin, and stained at room temperature using 0.5% crystal violet solution. All experiments were repeated at least three times.

Spheroid growth assay. The liquid overlay technique was used to grow melanoma spheroids (19). First, 96-well plates were coated with 50 μl of agar (1.25%) and 30 min later 25,000 melanoma cells (200 μl) were added to the wells. Spheroids were allowed to form and images were captured on the following day. The volume of the spheroids was calculated as follows: Volume=(4/3)π x b^2 x c, where b is the longest (semi-major) axis and c is the shortest (semi-minor) axis. All experiments were repeated at least three times.

Western blot analysis. Whole-cell lysates were prepared using the RIPA lysis buffer (cat. no. sc-24948A, Santa Cruz Biotechnology, Inc.) and collected via centrifugation at 12,800 x g at 4˚C for 30 min. Protein concentrations were determined using the Bradford method and 50 μg of the samples were denatured and loaded onto a 10% polyacrylamide gel. After separation, the proteins were transferred onto a polyvinylidene fluoride membrane, which was blocked with 5% non-fat milk for 1 h followed by overnight incubation with the primary antibody at 4˚C on a shaker. The membrane was then washed three times using PBS/0.05% Tween 20 and incubated with a horseradish peroxidase (HRP)-conjugated secondary antibody (Jackson ImmunoResearch Laboratories, cat. no. 111-035-003, dilution 1:2,500) for 1 h. All bands were detected using an ECL Western blot kit (Genesee, 20-302B). All experiments were repeated at least three times.

Immunohistochemistry. Paraffin-embedded sections of normal skin, nevus, or melanoma were dewaxed and gradually rehydrated before being immersed in an EDTA solution (pH 8.0) and heated using a pressure cooker for 2 min. After cooling to room temperature, the tissue sections were rinsed with PBS and normal goat serum was used to block non-specific binding. The tissue sections were then incubated with a mouse anti-human UCP2 monoclonal antibody (1:200 dilution) overnight at 4˚C. After washing with PBS, the tissue sections were incubated with an HRP-conjugated secondary antibody for 30 min at room temperature. The Ultraview Red agent was added to distinguish positive staining from skin pigmentation, and red particles deposited in the cytoplasm were considered as a positive result. Hematoxylin and eosin staining was performed separately to evaluate the pathological characteristics.

Semi-quantitative analysis of stained tissue sections. The stained sections were evaluated via double-blind scoring based on a slightly modified version of the procedure described by Bosman *et al* (20). Five different fields were randomly selected, and histochemical scores were calculated according to the positive rate of tumor cells [P(i)] and the staining intensity [S(i)] as follows:

$$\text{Histochemical score} = \frac{1}{5} \times [\sum_{i=1}^{i=5} P(i) \times S(i)]$$

In this equation, the P(i) is scored as 0 (no positive cells), 1 (<10% positive cells), 2 (10-50% positive cells), or 3 (>50% positive cells). The S(i) was scored as 0 (no staining), 1 (light yellow staining), 2 (brownish yellow staining), or 3 (red staining). The mean score for all 5 fields was calculated, and the result was graded as negative (-, score 0-1), mild (+, score 2-3), or strong (++, score ≥4).

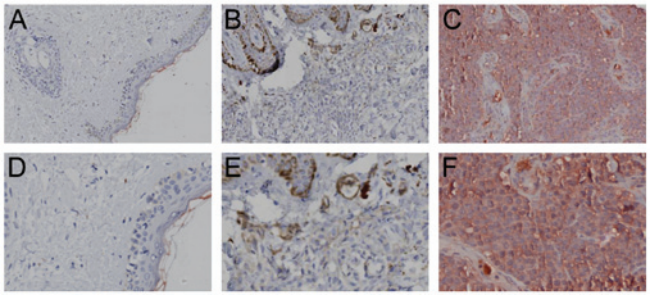

Figure 1. Immunohistochemical analysis demonstrated that UCP2 was more highly expressed in melanoma tissues compared with nevus tissues. Representative examples of (A and D) normal control tissue, (B and E) compound nevus tissues and (C and F) melanoma tissues. Ultraview Red agent was added to distinguish positive staining from skin pigmentation, with a positive result considered as red staining. Magnification: (A-C) x20, (D-F) x40. UCP2, uncoupling protein 2.

Statistical analysis. The statistical analyses were performed using the χ^2 test or analysis of variance as appropriate. One-way analysis of variance followed by Tukey-Kramer adjustment was used to examine differences between multiple groups. All statistical analyses were performed using SPSS software, version 13.0 (SPSS Inc.), and the results were considered statistically significant at P-values of <0.05.

Results

Associations between UCP2 expression and clinical characteristics of melanoma. Immunohistochemistry was used to evaluate UCP2 expression in the tissue specimens from the melanoma group (n=65), the compound nevus group (n=51) and the control group (n=49). As shown in Fig. 1, the red particles deposited in the cytoplasm indicate a positive result and the quantified results are presented in Table I. The UCP2 positivity rates were low in normal skin tissue (2.0%) and compound nevus tissue (5.9%), but relatively high in melanoma tissue (76.9%).

It was also evaluated whether UCP2 expression was correlated with Clark level and Breslow thickness (depth of invasion), lymph node infiltration and presence of ulceration. As summarized in Table II, UCP2 expression increased with the Clark level (P<0.001) and was significantly correlated with Breslow thickness (P=0.0235), but was not significantly correlated with lymph node infiltration status or the presence of ulceration.

UCP2 KD suppresses melanoma cell growth and induces cisplatin sensitivity. As UCP2 was more highly expressed in melanoma tissues compared with nevus tissues, it was further evaluated whether inhibiting UCP2 expression could suppress melanoma cell growth and sensitize these cells to cisplatin. Two widely used melanoma cell lines, A375 and SK-Mel-28, were infected using the control or UCP2 shRNA-containing lentivirus. After antibiotic selection, control lentivirus-infected cells (LC) and two stable UCP2 KD clones were established

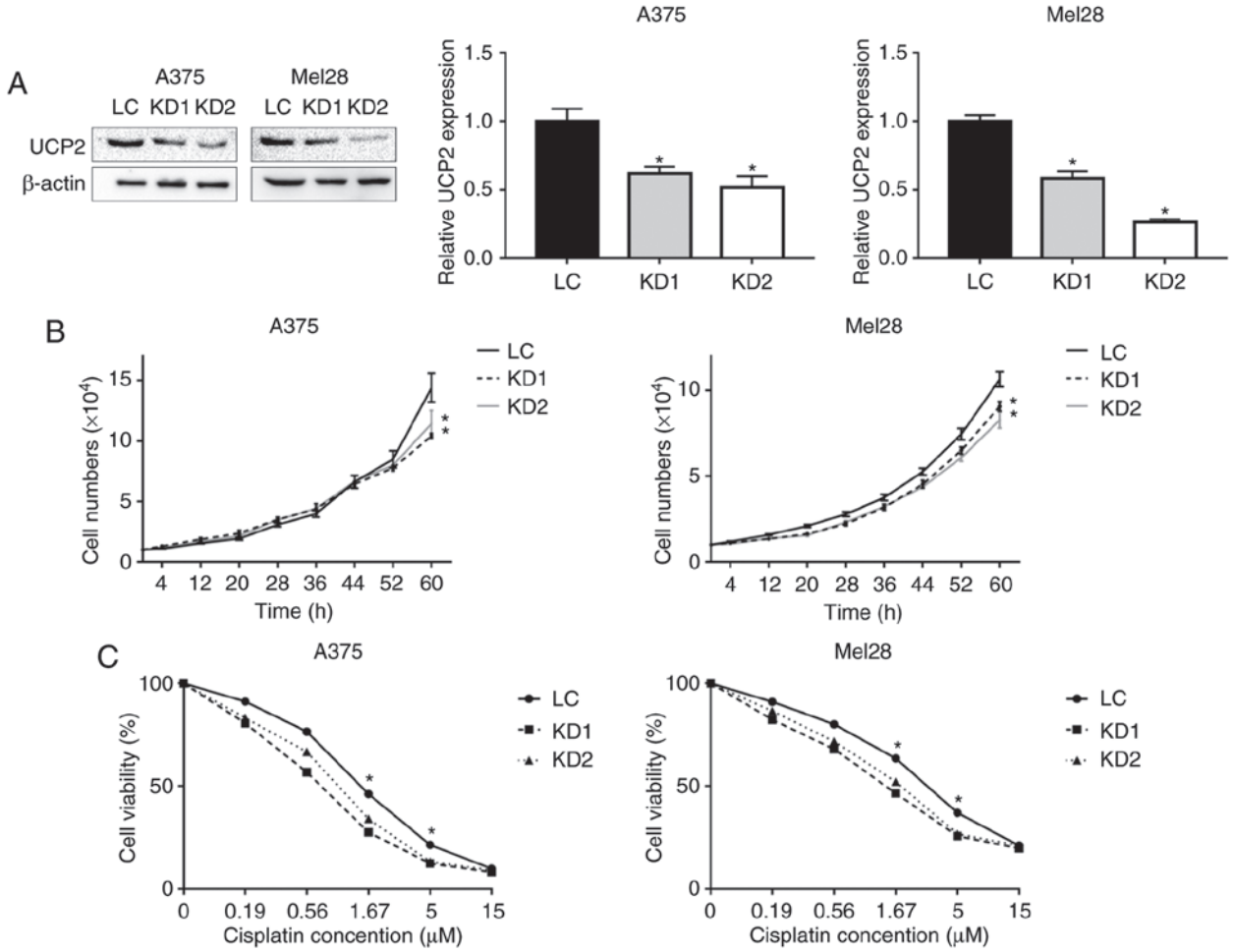

Figure 2. Inhibition of UCP2 suppresses melanoma cell growth and increases sensitivity to cisplatin. (A) Establishment of UCP2 stable knockdown clones. (B) Inhibition of UCP2 suppressed melanoma cell growth (n=6 each sample). (C) Inhibition of UCP2 also increased the sensitivity of melanoma cells to cisplatin (n=6 each sample). UCP2, uncoupling protein 2; LC, control lentivirus-infected cells; KD, UCP2 knockdown clones. Data are presented as mean ± standard deviation. *P<0.05 compared with the lentivirus control samples.

in each cell line (Fig. 2A). The UCP2 protein levels were reduced by 40-50% in the A375 KD clones and by 50-70% in the Mel-28 KD clones. As shown in Fig. 2B, after growing for 60 h, the proportion of cell growth was 72.4 and 79.3% for the A375 clones, relative to the control cells. For the SK-Mel-28 cells, the proportion of cell growth was 81.2 and 73.8%, relative to the control cells.

The cell viability assay was used to test sensitivity to cisplatin, which is a common chemotherapeutic agent used for the treatment of melanoma (18). The UCP2 KD and control cells were treated using different concentrations of cisplatin for 48 h, and cell viability was measured using the MTT assay. As shown in Fig. 2C, the UCP2 KD cells were more sensitive to cisplatin at concentrations of 1.67 and 5 μM. For example, at a concentration of 1.67 μM, the viability of A375 UCP2 KD clones was ~30% (vs. 46% for the control cells) and the viability of SK-Mel-28 UCP2 KD cells was ~49% (vs. 64% for the control cells). These results indicate that UCP2 inhibition increased the sensitivity of melanoma cells to cisplatin.

UCP2 inhibition decreases the mitochondrial membrane potential and the levels of ATP, H_2O_2 and lactate. As an uncoupling protein, UCP2 regulates the mitochondrial membrane potential, ATP synthesis and ROS generation (21). The JC-1 dye was used to examine the effects of UCP2 inhibition on the membrane potential ($\Delta\Psi$m), and the UCP2 KD clones exhibited increases in the membrane potential of 40-65% for the A375 and SK-Mel-28 cells (Fig. 3A). However, the increased membrane potential did not result in increased ATP generation, with ATP levels decreasing by 30-60% in the A375 and SK-Mel-28 UCP2 KD cells (Fig. 3B). As shown in Fig. 3C, the H_2O_2 levels were also decreased by 25-40% in the A375 and SK-Mel-28 UCP2 KD cells (Fig. 3C).

Glycolysis is often enhanced in tumor cells for ATP production and anabolism, which leads to increased lactate levels (22). However, in the A375 and SK-Mel-28 UCP2 KD cells, the lactate levels were decreased by 20-30% (Fig. 3D). These results suggested that inhibiting UCP2 reduced the rate of glycolysis and ATP generation in melanoma cells.

UCP2 inhibition suppresses melanoma cell invasion and three-dimensional growth. Malignant melanoma is an invasive tumor, and the Matrigel invasion assay was used to examine whether UCP2 inhibition affected cell migration and invasion. As shown in Fig. 4A and B, after a 12-h incubation, only 60-75% of the A375 UCP2 KD cells had migrated through

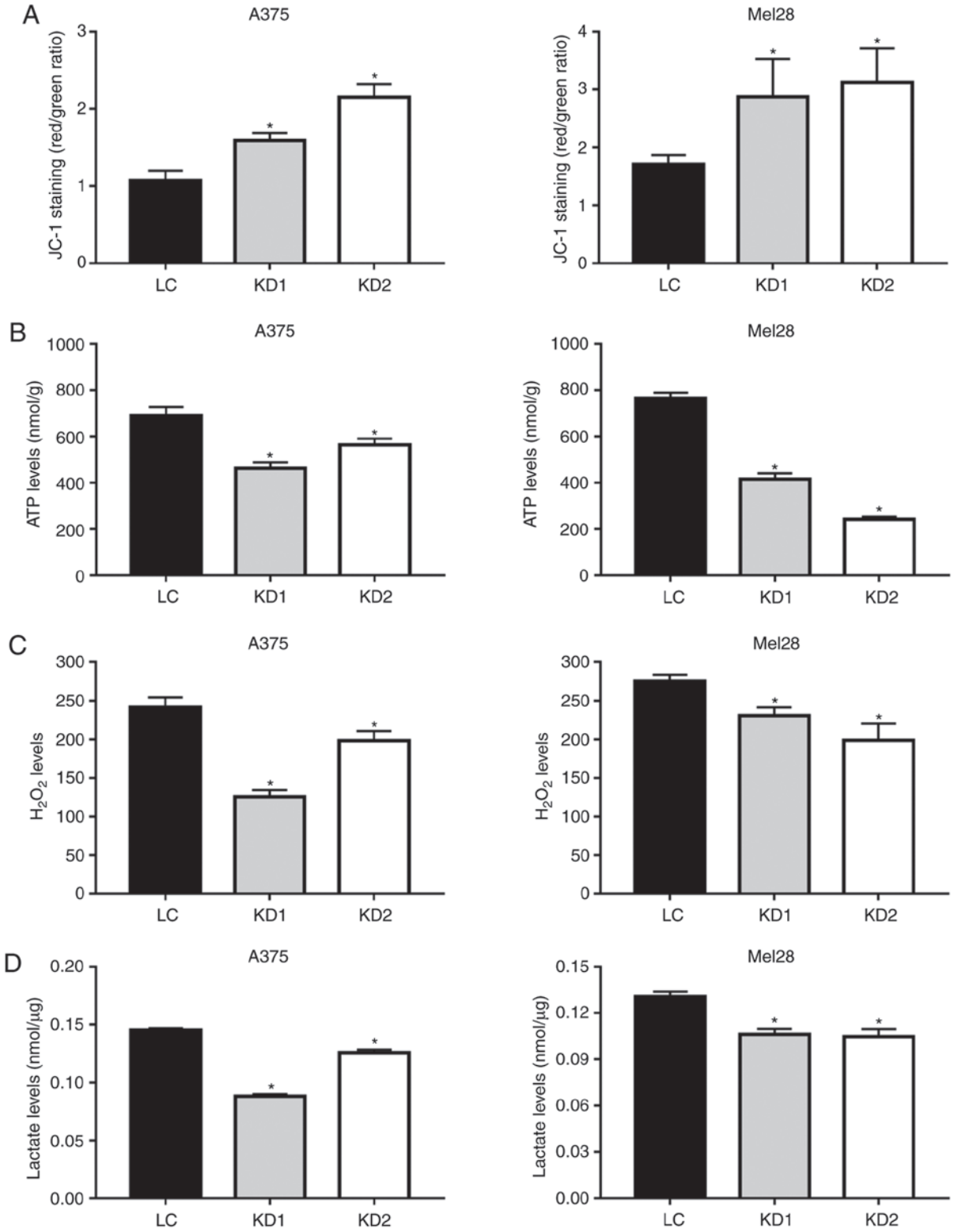

Figure 3. Inhibition of UCP2 negatively affects energy metabolism in melanoma cells. (A) Mitochondrial membrane potential was increased in UCP2 KD melanoma cells. (B) Generation of ATP was suppressed in UCP2 KD melanoma cells. (C) Intracellular H_2O_2 levels were decreased in UCP2 KD melanoma cells. (D) Intracellular lactate levels were decreased in UCP2 KD melanoma cells. Data are presented as mean ± standard deviation (n=6 each sample). *P<0.05 compared with the lentivirus control samples. LC, control lentivirus-infected cells; KD, UCP2 knockdown clones; UCP2, uncoupling protein 2.

the Matrigel (vs. the control A375 cells) and only 65-85% of the SK-Mel-28 UCP2 KD cells had migrated (vs. the control SK-Mel-28 cells). The three-dimensional spheroid growth assay was performed to evaluate the tumorigenicity of the UCP2 KD cells. For the SK-Mel-28 cells, the UCP2 KD cells formed spheroids with ~40% of the volume of the control cell spheroids (Fig. 4C and D). For the A375 cells, one UCP2 KD clone formed smaller spheroids compared with the control, while the other clone formed larger spheroids, but with markedly lower density based on fluorescence intensity analysis.

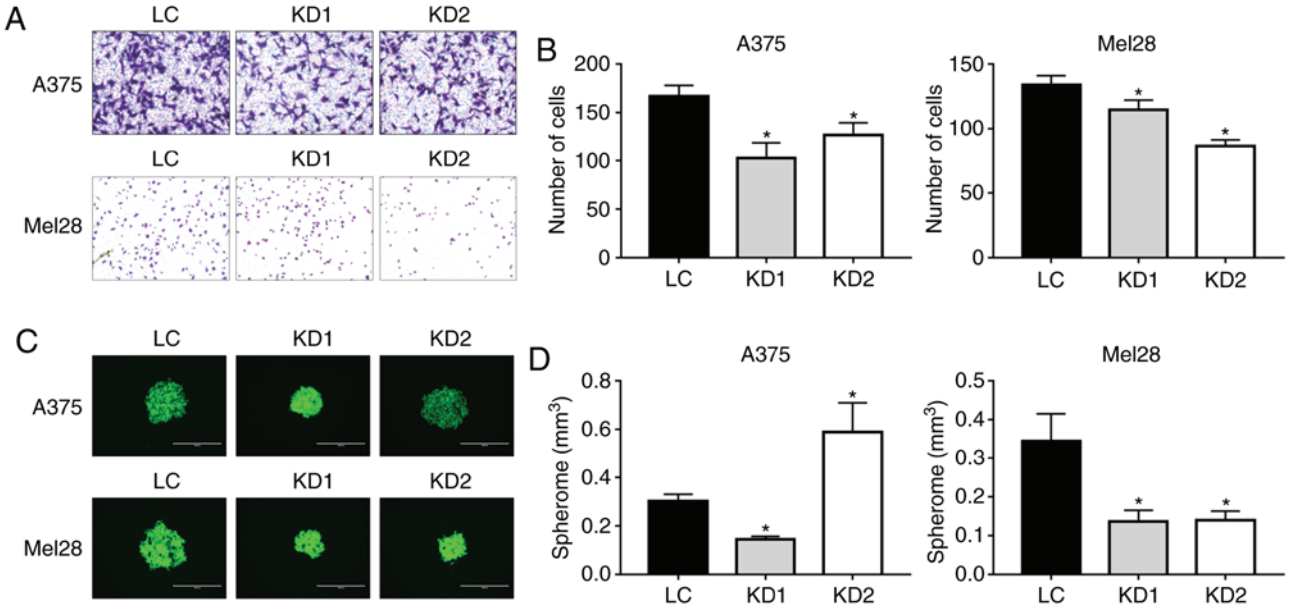

Figure 4. Inhibition of UCP2 suppresses melanoma cell invasion and clonal formation. (A) Staining and (B) quantification of invading melanoma cells in the Matrigel assay. (C) Visualizing and (D) quantification of spheroid volume formed by the melanoma cells. Data are presented as mean ± standard deviation (n=6 each sample). *P<0.05 compared with the lentivirus control samples. LC, control lentivirus-infected cells; KD, UCP2 knockdown clones; UCP2, uncoupling protein 2.

These results suggested that inhibition of UCP2 expression reduced the tumorigenicity of melanoma cells.

UCP2 inhibition suppresses Akt/mTOR and ERK signaling in melanoma cells. During melanomagenesis, Akt/mTOR signaling plays a key role in the regulation of cell proliferation, growth and apoptosis (23). Fig. 5A and B show the lower levels of phosphorylated Akt (Thr308) in both lines of UCP2 KD cells. As downstream effectors for mTOR, p70S6K and 4E-BP1 regulate cell growth and proliferation, and their activation is often associated with tumor development (24,25). Inhibition of UCP2 expression was found to be associated with significantly reduced levels of phosphorylated p70S6K (Thr389) and 4E-BP1 (Thr70) relative to the control cells (Fig. 5A, B and E). The expression of p70S6K was not significantly altered, although the expression of 4E-BP1 was increased in the A375 UCP2 KD cells, but not in the SK-Mel-28 UCP2 KD cells.

The ERK pathway also plays a crucial role in regulating melanoma cell proliferation, differentiation and apoptosis (26). The UCP2 KD clones in both cell lines exhibited significantly reduced levels of both phosphorylated ERK (Tyr204) and total ERK proteins, relative to the control cells (Fig. 5C and D); therefore, the p-ERK/ERK ratio was not decreased in the UCP2 KD clones (Fig. 5E). These results suggested that inhibition of UCP2 expression suppressed Akt/mTOR and ERK signaling in melanoma cells.

Discussion

The incidence of melanoma has continued to rise in recent years, which is a major cause of concern (27), as malignant melanoma is highly invasive and is difficult to cure after metastasis has occurred (28). The incidence of melanoma is affected by age and sex, with women having a higher incidence at younger ages and men having a higher incidence at older ages (29). These differences suggest that metabolic and hormone changes may affect the pathogenesis of melanoma. As an uncoupling protein, UCP2 is an important regulator of metabolism (7) and is often highly expressed in human cancers, where it promotes the shift from oxidative phosphorylation to glycolysis (11). Our earlier studies have demonstrated that UCP2 is highly expressed in non-melanoma skin cancers (30), although UCP2 knockout in a mouse model suppressed chemically-induced skin carcinogenesis (14). Furthermore, carcinogen treatment induced glycolysis, which was suppressed by the UCP2 knockout (14). Therefore, our earlier work was extended to focus on the role of UCP2 in human melanoma, which is the deadliest type of skin cancer.

To the best of our knowledge, this is the first study to evaluate whether UCP2 expression was correlated with melanoma's Clark level and Breslow thickness, which reflect the depth of invasion. As melanoma is one of the most aggressive and treatment-resistant cancers (3), the results suggest that UCP2 may contribute to melanoma's aggressiveness and that targeting UCP2 may suppress melanoma progression. This hypothesis was tested in UCP2 KD melanoma cells, and inhibition of UCP2 expression in human melanoma cells suppressed cell migration, invasion and three-dimensional spheroid growth (Fig. 4). Furthermore, the inhibition of UCP2 expression sensitized melanoma cells to cisplatin (Fig. 2C). The fact that inhibition of UCP2 expression decreased the membrane potential is consistent with its role as an uncoupling protein. Moreover, the reduced lactate levels and ATP production in UCP2 KD cells suggest that glycolysis was inhibited, which is also consistent with the role of UCP2 in shifting metabolism towards glycolysis (11).

Several key signaling pathways contribute to melanoma aggressiveness, including the MARK and Akt pathways. As one

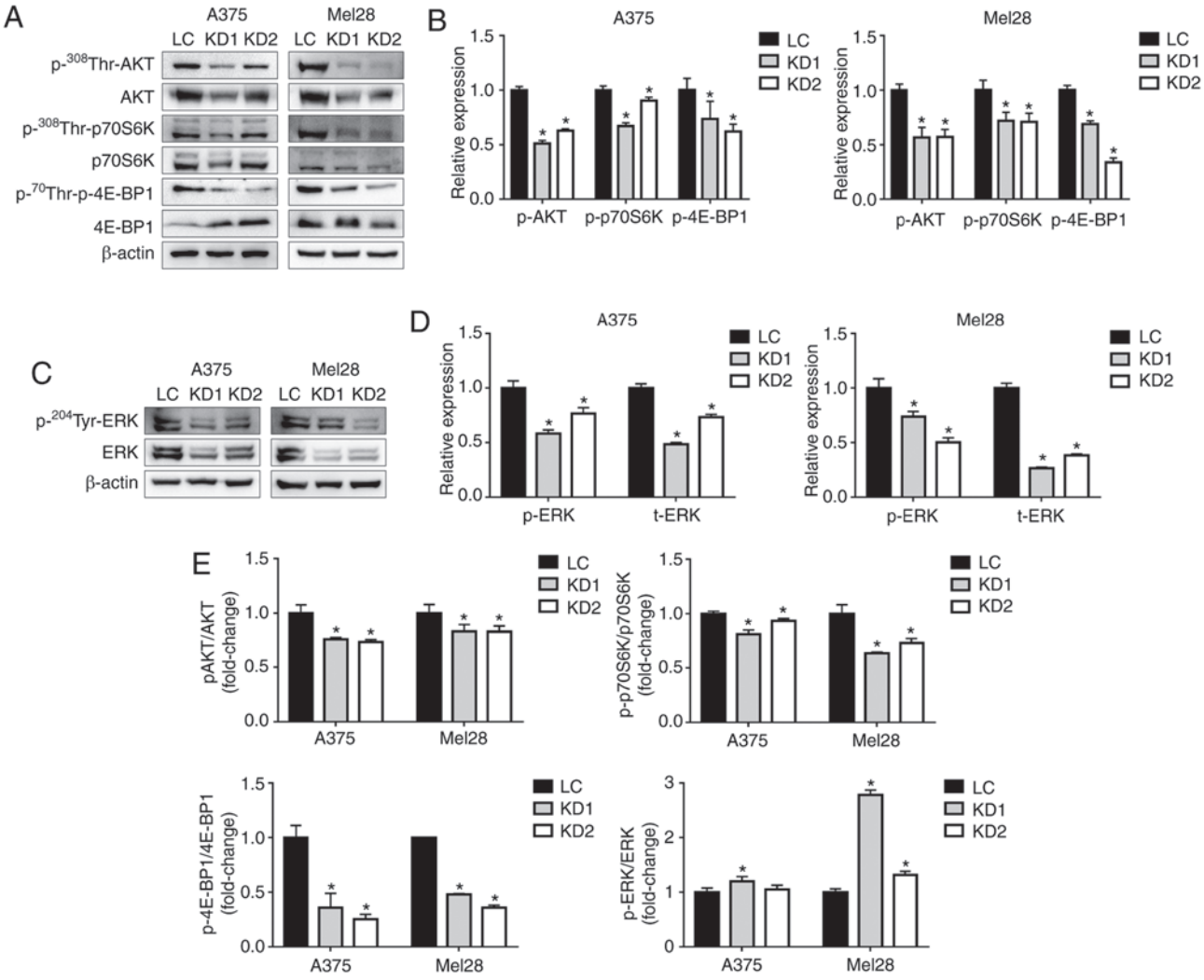

Figure 5. Inhibition of UCP2 inactivates the Akt/mTOR and ERK kinases in melanoma cells. (A) Detection and (B and E) quantification of (p)AKT, (p)p70S6K, and (p)4E-BP1 in melanoma cells. (C) Detection and (D and E) quantification of (p)ERK in melanoma cells. Data are presented as mean ± standard deviation. *P<0.05 compared with the lentivirus control samples. LC, control lentivirus-infected cells; KD, UCP2 knockdown clones; UCP2, uncoupling protein 2; Akt, protein kinase B; mTOR, mammalian target of rapamycin; ERK, extracellular signal-regulated kinase.

of the main arms of the MAPK pathway, Ras/Raf/MEK/ERK play a vital role in melanomagenesis (31), with the signal cascade culminating in ERK1/2 and activating downstream transcription factors, thereby contributing to melanoma cell proliferation and migration (31,32). Inhibition of UCP2 expression inactivated ERK, suggesting that tumor suppression may be achieved in melanoma cells by targeting UCP2 (Fig. 5C).

The activation of Akt is another important pathway in melanomagenesis (33), which contributes to stimulating ROS generation and DNA mutation (34), promoting drug resistance (35), and promoting metastasis to the lung and brain (36), as well as being associated with poor survival (37). Activated Akt transduces signals through a number of target proteins, including mTOR, and mTOR stimulates protein synthesis via effectors p70S6K and p4E-BP1 (38). As a serine/threonine protein kinase, mTOR also plays an oncogenic role in several human cancers, including melanoma, where mTOR activation promotes melanoma cell proliferation and invasiveness (39). Moreover, inhibition of Akt/mTOR greatly increases the sensitivity of melanoma cells to chemotherapy (e.g., cisplatin or temozolomide) (40). The present study also revealed that inhibition of UCP2 resulted in lower levels of phosphorylated Akt, phosphorylated p70S6K and phosphorylated 4E-BP1, which suggests that UCP2 promotes the Akt/mTOR pathway in melanoma cells. Similar results have been observed in breast cancer cells, where upregulated UCP2 was shown to activate the PI3K/Akt/mTOR pathway and lead to increased tumor autophagy, which is responsible for drug resistance (41).

In remains unclear how UCP2 promotes ERK and Akt/mTOR signaling in melanoma cells. However, the present study revealed that UCP2 KD cells exhibited lower levels of ROS (H_2O_2), which contrasts with the generally elevated H_2O_2 levels in cancer cells (42). There is a variety of factors contributing to the production of H_2O_2 in cancer cells, which promotes cancer cell metabolism, proliferation and metastasis (43). Furthermore, both ERK and Akt/mTOR are activated by elevated ROS levels (12,13). Therefore, the decreased H_2O_2 levels in UCP2 KD cells may contribute to downregulation of Akt/mTOR and ERK signaling, although the precise underlying mechanism remains unclear.

There were several limitations to the present study. First, paradoxical roles have been reported for UCP2 in tumorigenesis

and there is controversy regarding its role in melanoma (44). Second, ethnicity-related differences may help explain the differences in certain clinical characteristics, and variations in cell lines and genetic techniques (e.g., UCP2 overexpression or KD) may also account for some of the differences observed during *in vitro* studies. However, the findings of the present study suggest that UCP2 KD in melanoma cells conferred a treatment benefit, which raises the possibility that UCP2 may be a useful target for adjuvant therapy.

To the best of our knowledge, this is the first report of UCP2 being more highly expressed in human melanoma tissues compared with compound nevus tissues. In addition, the level of UCP2 expression was found to be correlated with tumor grade and depth of invasion. Furthermore, inhibition of UCP2 expression inactivated the Akt/mTOR and ERK pathways, which may be responsible for the observed decrease in cell proliferation and invasion, as well as increase in sensitivity to cisplatin treatment. Further studies are required to analyze the mRNA expression of UCP2 in tissue samples, in order to evaluate the effects of drugs that target UCP2 and Akt/mTOR/ERK, which may represent a novel treatment strategy for melanoma.

Acknowledgements

The IncuCyte Live Cell Analysis system was provided by the Feist-Weiller Cancer Center's Innovative North Louisiana Experimental Therapeutics program (INLET), which is directed by Dr Glenn Mills at LSUHSC-Shreveport and supported by the LSU Health Shreveport Foundation. The authors would like to thank Dr Ana-Maria Dragoi (Associate Director of INLET), Dr Jennifer Carroll (Director of the *In vivo*, *In vitro* Efficacy Core), and Reneau Youngblood (Research Associate) for their assistance with the IncuCyte experiments. Flow cytometry experiments were performed by David Custis at the institutional Research Core Facility.

Funding

The present study was supported by funds from the Department of Pharmacology, Toxicology and Neuroscience, LSU Health Sciences Center in Shreveport.

Availability of data and materials

All the datasets generated and analyzed during the present study are available from the corresponding author on reasonable request.

Authors' contributions

Study design: JL, CN, XC and YZ. Data collection and analysis: JL, YJ, LA and CN. Manuscript preparation: JL, CN, XC and YZ.

Ethics approval and consent to participate

The protocol of this retrospective study was approved by the Institutional Review Board of China-Japan Union Hospital, Jilin University. Informed consent was obtained from patients at the time of sample collection.

Patient consent for publication

Not applicable.

Competing interests

The authors declare that they have no competing interests.

References

1. Linares MA, Zakaria A and Nizran P: Skin cancer. Prim Care 42: 645-659, 2015.
2. Haenssle HA, Mograby N, Ngassa A, Buhl T, Emmert S, Schön MP, Rosenberger A and Bertsch HP: Association of patient risk factors and frequency of nevus-associated cutaneous melanomas. JAMA Dermatol 152: 291-298, 2016.
3. Tsao H, Chin L, Garraway LA and Fisher DE: Melanoma: From mutations to medicine. Genes Dev 26: 1131-1155, 2012.
4. Moon H, Donahue LR, Choi E, Scumpia PO, Lowry WE, Grenier JK, Zhu J and White AC: Melanocyte stem cell activation and translocation initiate cutaneous melanoma in response to UV exposure. Cell Stem Cell 21: 665-678, 2017.
5. Ježek P, Holendová B, Garlid KD and Jabůrek M: Mitochondrial uncoupling Proteins: Subtle regulators of cellular redox signaling. Antioxid Redox Signal 29: 667-714, 2018.
6. Rial E, González-Barroso MM, Fleury C and Bouillaud F: The structure and function of the brown fat uncoupling protein UCP1: Current status. Biofactors 8: 209-219, 1998.
7. Toda C and Diano S: Mitochondrial UCP2 in the central regulation of metabolism. Best Pract Res Clin Endocrinol Metab 28: 757-764, 2014.
8. Boss O, Samec S, Paoloni-Giacobino A, Rossier C, Dulloo A, Seydoux J, Muzzin P and Giacobino JP: Uncoupling protein-3: A new member of the mitochondrial carrier family with tissue-specific expression. FEBS Lett 408: 39-42, 1997.
9. Mao W, Yu XX, Zhong A, Li W, Brush J, Sherwood SW, Adams SH and Pan G: UCP4, a novel brain-specific mitochondrial protein that reduces membrane potential in mammalian cells. FEBS Lett 443: 326-330, 1999.
10. Yu XX, Mao W, Zhong A, Schow P, Brush J, Sherwood SW, Adams SH and Pan G: Characterization of novel UCP5/BMCP1 isoforms and differential regulation of UCP4 and UCP5 expression through dietary or temperature manipulation. FASEB J 14: 1611-1618, 2000.
11. Brandi J, Cecconi D, Cordani M, Torrens-Mas M, Pacchiana R, Dalla Pozza E, Butera G, Manfredi M, Marengo E, Oliver J, *et al*: The antioxidant uncoupling protein 2 stimulates hnRNPA2/B1, GLUT1 and PKM2 expression and sensitizes pancreas cancer cells to glycolysis inhibition. Free Radic Biol Med 101: 305-316, 2016.
12. Elorza A, Hyde B, Mikkola HK, Collins S and Shirihai OS: UCP2 modulates cell proliferation through the MAPK/ERK pathway during erythropoiesis and has no effect on heme biosynthesis. J Biol Chem 283: 30461-30470, 2008.
13. Dando I, Pacchiana R, Pozza ED, Cataldo I, Bruno S, Conti P, Cordani M, Grimaldi A, Butera G, Caraglia M, *et al*: UCP2 inhibition induces ROS/Akt/mTOR axis: Role of GAPDH nuclear translocation in genipin/everolimus anticancer synergism. Free Radic Biol Med 113: 176-189, 2017.
14. Li W, Zhang C, Jackson K, Shen X, Jin R, Li G, Kevil CG, Gu X, Shi R and Zhao Y: UCP2 knockout suppresses mouse skin carcinogenesis. Cancer Prev Res (Phila) 8: 487-491, 2015.
15. Sreedhar A, Petruska P, Miriyala S, Panchatcharam M and Zhao Y: UCP2 overexpression enhanced glycolysis via activation of PFKFB2 during skin cell transformation. Oncotarget 8: 95504- 95515, 2017.
16. Sreedhar A, Lefort J, Petruska P, Gu X, Shi R, Miriyala S, Panchatcharam M and Zhao Y: UCP2 upregulation promotes Plcγ-1 signaling during skin cell transformation. Mol Carcinog 56: 2290-2300, 2017.
17. Rossi S, Cordella M, Tabolacci C, Nassa G, D'Arcangelo D, Senatore C, Pagnotto P, Magliozzi R, Salvati A, Weisz A, *et al*: TNF-alpha and metalloproteases as key players in melanoma cells aggressiveness. J Exp Clin Cancer Res 37: 326, 2018
18. Bhatia S, Tykodi SS and Thompson JA: Treatment of metastatic melanoma: An overview. Oncology (Williston Park) 23: 488-496, 2009.

19. Rofstad EK, Wahl A, Davies Cde L and Brustad T: Growth characteristics of human melanoma multicellular spheroids in liquid-overlay culture: Comparisons with the parent tumour xenografts. Cell Tissue Kinet 19: 205-216, 1986.
20. Bosman FT, de Goeij AF and Rousch M: Quality control in immunocytochemistry: Experiences with the oestrogen receptor assay. J Clin Pathol 45: 120-124, 1992.
21. Baffy G, Derdak Z and Robson SC: Mitochondrial recoupling: A novel therapeutic strategy for cancer? Br J Cancer 105: 469-474, 2011.
22. Gill KS, Fernandes P, O'Donovan TR, McKenna SL, Doddakula KK, Power DG, Soden DM and Forde PF: Glycolysis inhibition as a cancer treatment and its role in an anti-tumour immune response. Biochim Biophys Acta 1866: 87-105, 2016.
23. Pópulo H, Lopes JM and Soares P: The mTOR signalling pathway in human cancer. Int J Mol Sci 13: 1886-1918, 2012.
24. Calero R, Morchon E, Martinez-Argudo I and Serrano R: Synergistic anti-tumor effect of 17AAG with the PI3K/mTOR inhibitor NVP-BEZ235 on human melanoma. Cancer Lett 406: 1-11, 2017.
25. Babchia N, Calipel A, Mouriaux F, Faussat AM and Mascarelli F: The PI3K/Akt and mTOR/P70S6K signaling pathways in human uveal melanoma cells: Interaction with B-Raf/ERK. Invest Ophthalmol Vis Sci 51: 421-429, 2010.
26. Mao XH, Chen M, Wang Y, Cui PG, Liu SB and Xu ZY: MicroRNA-21 regulates the ERK/NF-κB signaling pathway to affect the proliferation, migration, and apoptosis of human melanoma A375 cells by targeting SPRY1, PDCD4, and PTEN. Mol Carcinog 56: 886-894, 2017.
27. Siegel RL, Miller KD and Jemal A: Cancer statistics, 2017. CA Cancer J Clin 67: 7-30, 2017.
28. Eggermont AM, Spatz A and Robert C: Cutaneous melanoma. Lancet 383: 816-827, 2014.
29. Rigel DS: Epidemiology of melanoma. Semin Cutan Med Surg 29: 204-209, 2010.
30. Li W, Nichols K, Nathan CA and Zhao Y: Mitochondrial uncoupling protein 2 is up-regulated in human head and neck, skin, pancreatic, and prostate tumors. Cancer Biomark 13: 377-383, 2013.
31. Estrada Y, Dong J and Ossowski L: Positive crosstalk between ERK and p38 in melanoma stimulates migration and in vivo proliferation. Pigment Cell Melanoma Res 22: 66-76, 2009.
32. Dhillon AS, Hagan S, Rath O and Kolch W: MAP kinase signalling pathways in cancer. Oncogene 26: 3279-3290, 2007.
33. Altomare DA and Testa JR: Perturbations of the AKT signaling pathway in human cancer. Oncogene 24: 7455-7464, 2005.
34. Govindarajan B, Sligh JE, Vincent BJ, Li M, Canter JA, Nickoloff BJ, Rodenburg RJ, Smeitink JA, Oberley L, Zhang Y, *et al*: Overexpression of Akt converts radial growth melanoma to vertical growth melanoma. J Clin Invest 117: 719-729, 2007.
35. Niessner H, Forschner A, Klumpp B, Honegger JB, Witte M, Bornemann A, Dummer R, Adam A, Bauer J, Tabatabai G, *et al*: Targeting hyperactivation of the AKT survival pathway to overcome therapy resistance of melanoma brain metastases. Cancer Med 2: 76-85, 2013.
36. Cho JH, Robinson JP, Arave RA, Burnett WJ, Kircher DA, Chen G, Davies MA, Grossmann AH, VanBrocklin MW, McMahon M and Holmen SL: AKT1 activation promotes development of melanoma metastases. Cell Rep 13: 898-905, 2015.
37. Dai DL, Martinka M and Li G: Prognostic significance of activated Akt expression in melanoma: A clinicopathologic study of 292 cases. J Clin Oncol 23: 1473-1482, 2005.
38. Polivka Jr J and Janku F: Molecular targets for cancer therapy in the PI3K/AKT/mTOR pathway. Pharmacol Ther 142: 164-175, 2014.
39. Yang Y, Luo Z, Hao Y, Ba W, Wang R, Wang W, Ding X and Li C: mTOR-mediated Na+/Ca2+ exchange affects cell proliferation and metastasis of melanoma cells. Biomed Pharmacother 92: 744-749, 2017.
40. Sinnberg T, Lasithiotakis K, Niessner H, Schittek B, Flaherty KT, Kulms D, Maczey E, Campos M, Gogel J, Garbe C and Meier F: Inhibition of PI3K-AKT-mTOR signaling sensitizes melanoma cells to cisplatin and temozolomide. J Invest Dermatol 129: 1500-1515, 2009.
41. Yu X, Luo A, Liu Y, Wang S, Li Y, Shi W, Liu Z and Qu X: MiR-214 increases the sensitivity of breast cancer cells to tamoxifen and fulvestrant through inhibition of autophagy. Mol Cancer 14: 208, 2015.
42. Szatrowski TP and Nathan CF: Production of large amounts of hydrogen peroxide by human tumor cells. Cancer Res 51: 794-798, 1991.
43. Lisanti MP, Martinez-Outschoorn UE, Lin Z, Pavlides S, Whitaker-Menezes D, Pestell RG, Howell A and Sotgia F: Hydrogen peroxide fuels aging, inflammation, cancer metabolism and metastasis: The seed and soil also needs 'fertilizer'. Cell Cycle 10: 2440-2449, 2011.
44. Cheng WC, Tsui YC, Ragusa S, Koelzer VH, Mina M, Franco F, Läubli H, Tschumi B, Speiser D, Romero P, *et al*: Uncoupling protein 2 reprograms the tumor microenvironment to support the anti-tumor immune cycle. Nat Immunol 20: 206-217, 2019.